JPEDAV (2015) 36:592–598
DOI: 10.1007/s11669-015-0407-1
1547-7037 ©ASM International

Experimental Investigation of the Phase Equilibria in the Co-Nb-V Ternary System

C.P. Wang, S. Yang, S.Y. Yang, D. Wang, J.J. Ruan, J. Li, and X.J. Liu

(Submitted May 11, 2015; in revised form August 9, 2015; published online October 19, 2015)

Phase relationships in the Co-Nb-V ternary system were experimentally examined through electron probe microanalyzer and x-ray diffraction, and the isothermal sections of 1000 and 1200 °C were established. The obtained experimental results also show: (1) the (Nb, V) phase forms the continuous solid solution; (2) niobium solutes into α (Co) and σ-Co_2V_3 phases with a small solubility; (3) the C36 Laves-phase is stabilized at 1000 °C which is below its stability limits in Co-Nb binary system, and it forms a single phase region at 1000 °C; (4) vanadium has a large solubility in C36 Laves-phase; (5) vanadium and cobalt atoms show the analogous site occupation in C36 Laves-phase.

Keywords Co-Nb-V ternary system, isothermal section, phase relationship, solubility

1. Introduction

The γ′ phase with ordered $L1_2$ structure is discovered in the Co-Al-W-base alloys,[1] which show the same strengthening mechanism as the commonly used Ni-base superalloys reinforced by this phase. Thus, the Co-Al-W-base high-temperature alloys show potential applications in the field of aircraft turbines and combustor sections etc. However, the γ′ phase is not stable in the alloys. Some elements, Nb, Ta, Mo, Ti and V, are respectively incorporated into γ′ phase in the Co-Al-W system to improve its thermal stability,[2] as well as improve the performance of Co-base high-temperature materials[3-5] and magnetic materials.[6-8] For example, alloying with vanadium enhances the ductility, strength, and corrosion resistance of materials,[9] addition refractory elements, such as Nb, is one of the most efficient methods to improve high-temperature strength through the solid-solution strengthening.[10] It is important to understand the phase relationship of Co-Nb-V ternary system. However, there are no reports corresponding to this system. Based on EPMA and XRD, the purpose of this study is to determine the phase relationship in the Co-Nb-V ternary system at two isothermal sections (1000 and 1200 °C). The results obtained in the present work is expected to give a better understanding of the microstructure in the Co-Nb-V alloys for its practical applications, and it also benefits the thermodynamic assessment of Co-Nb-V ternary system.

The binary Co-V system has been investigated extensively by many authors.[11-17] The result calculated by Bratberg and Sundman[18] is consistent with existing experimental data. There are three intermetallic compounds in the Co-V system that is Co_3V, σ-Co_2V_3 and CoV_3. The phase diagram of the Co-Nb system has been studied in some investigations,[19-32] which was revised by Stein.[33] Five intermediate phases exist in the Co-Nb binary system namely C14, C15, C36, Co_7Nb_2 and Co_7Nb_6, respectively. The Nb-V system was assessed by Kumar.[34] The phase diagrams of Co-V,[18] Co-Nb,[33] and Nb-V[34] that constitute the Co-Nb-V ternary system are shown in Fig. 1. The stable solid phases and their crystal structures in the three binary systems in Co-Nb-V ternary system are listed in Table 1.

2. Experimental Procedures

The Cobalt (99.9 wt.%), Niobium (99.7 wt.%) and Vanadium (99.7 wt.%) were used as raw materials. Bulk alloys were prepared from pure elements by arc melting under high purity argon atmosphere. The ingots, weighting around 20 g, were melted at least 5 times in order to achieve the homogeneity of the sample. Each ingot was cut into small pieces by wire-cutting machine for heat treatment.

The vacuum in the quartz capsule containing the plate-shaped specimen was pumped to 5 Pa. And then, the evacuated capsule was filled with argon to a certain pressure. Furthermore, in order to avoid oxidation of samples, the above processes were repeated for four times. The specimens in quartz capsules were annealed at 1000 and 1200 °C followed by ice water quenching. The time of the heat treatment are 45 days at 1000 °C and 25 days at 1200 °C, respectively.

After metallographic preparation, the microstructure observation and the equilibrium composition measurement of each phase in the specimens were carried by electron probe microanalyzer (EPMA, JXA-8100, JEOL, Japan, the accelerating voltage and probe current were 20 kV and 1.0×10^{-8} A, respectively). The adopted composition was

C.P. Wang, S.Y. Yang, and X.J. Liu, Department of Materials Science and Engineering, College of Materials, Xiamen University, Xiamen, 361005, P.R. China and Research Center of Materials Design and Applications, Xiamen University, Xiamen, 361005, P.R. China; and **S. Yang, D. Wang, J.J. Ruan,** and **J. Li**, Department of Materials Science and Engineering, College of Materials, Xiamen University, Xiamen, 361005, P.R. China. Contact e-mail: lxj@xmu.edu.cn.

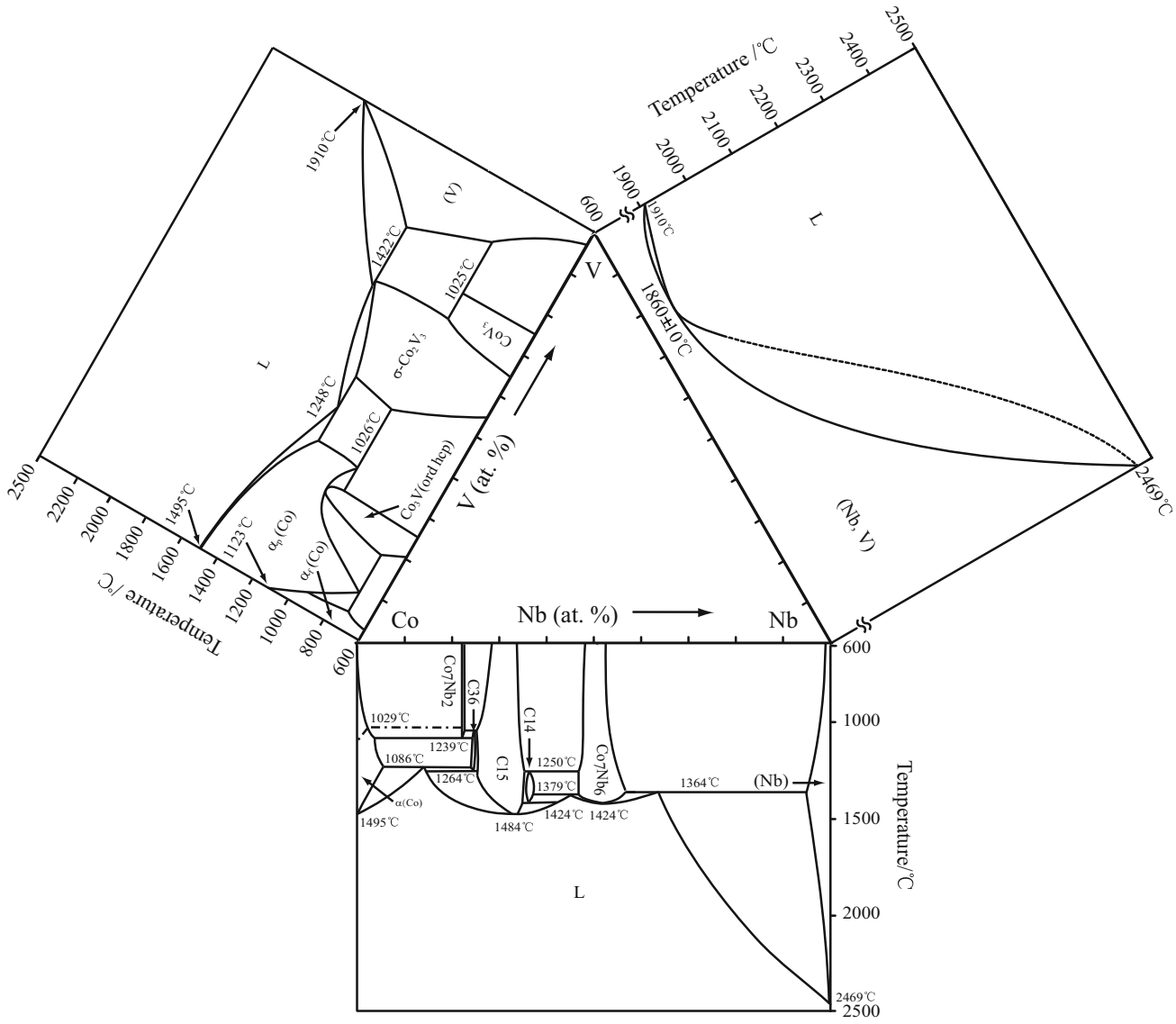

Fig. 1 Binary phase diagrams constituting the Co-Nb-V ternary system[18,33,34]

determined by the mean value of five measurements which were calibrated by the ZAF (Z: atomic number effect, A: absorption effect, F: fluorescence effect) correction, using pure elements as standard samples. The XRD measurement was carried out on a Philips Panalytical X-pert diffractometer using Cu Kα radiation at 40 kV and 30 mA. The data were collected in the range of 2θ from 20° to 90° at a step size of 0.0167°.

3. Results and Discussion

3.1 Microstructure and Phase Equilibria

Back-scattered electron (BSE) images of the typical ternary Co-Nb-V alloys are illustrated in Fig. 2(a)-(f), and the XRD results of the typical Co-Nb-V ternary alloys are presented in Fig. 3(a)-(c). For comparison, the standard XRD patterns of each phase (σ-Co_2V_3, Co_3V, C36, (Nb, V) and Co_7Nb_6) noted by different color vertical lines are shown in Fig. 3(a)-(c) as well. Phase identification is based on the equilibrium composition measured by EPMA and crystal structure confirmed by XRD analysis.

The two-phase equilibrium (Co_7Nb_2 + α (Co)) was identified in the $Co_{85}Nb_{10}V_5$ (here-after, alloy compositions are indicated in at.%) alloy annealed at 1000 °C for 45 days. White regions and light gray regions in Fig. 2(a) represent Co_7Nb_2 and α (Co) phases, respectively. In the $Co_{75}Nb_{10}V_{15}$ alloy after annealing at 1000 °C for 45 days, the two-phase equilibrium (Co_3V (light gray) + C36 (white)) was investigated, as shown in Fig. 2(b). In the

Table 1 The stable solid phases in the Co-Nb-V binary systems

System	Phase	Pearson's symbol	Prototype	Space group	Strukturbericht	References
Co-V	α (Co)	*cF*4	Cu	*Fm*-3 *m*	A1	[18]
	ε (Co)	*hP*2	Mg	*P*6$_3$/*mmc*	A3	[18]
	Co_3V	*hP*24	Mg_3Cr	*P*-6*m*2	Co_3V	[18]
	σ-Co_2V_3	*tP*30	σCrFe	*P*4$_2$/*mnm*	D8$_6$	[18]
	CoV_3	*cP*8	Cr_3Si	*Pm*-3*n*	A15	[18]
	(V)	*cI*2	W	*Im*-3 *m*	A2	[18]
Co-Nb	α (Co)	*cF*4	Cu	*Fm*-3 *m*	A1	[33]
	ε (Co)	*hP*2	Mg	*P*6$_3$/*mmc*	A3	[33]
	Co_7Nb_2	…	…	…	…	[33]
	α-Co_2Nb	*hP*24	$MgNi_2$	*P*6$_3$/*mmc*	C36	[33]
	γ-Co_2Nb	*cF*24	$MgCu_2$	*Fd*-3 *m*	C15	[33]
	β-Co_2Nb	*hP*12	$MgZn_2$	*P*6$_3$/*mmc*	C14	[33]
	Co_7Nb_6	*hR*13	Fe_7W_6	*R*-3 *m*	D85	[33]
	(Nb)	*cI*2	W	*Im*-3 *m*	A2	[33]
Nb-V	(Nb, V)	*cI*2	W	*Im*-3 *m*	A2	[34]

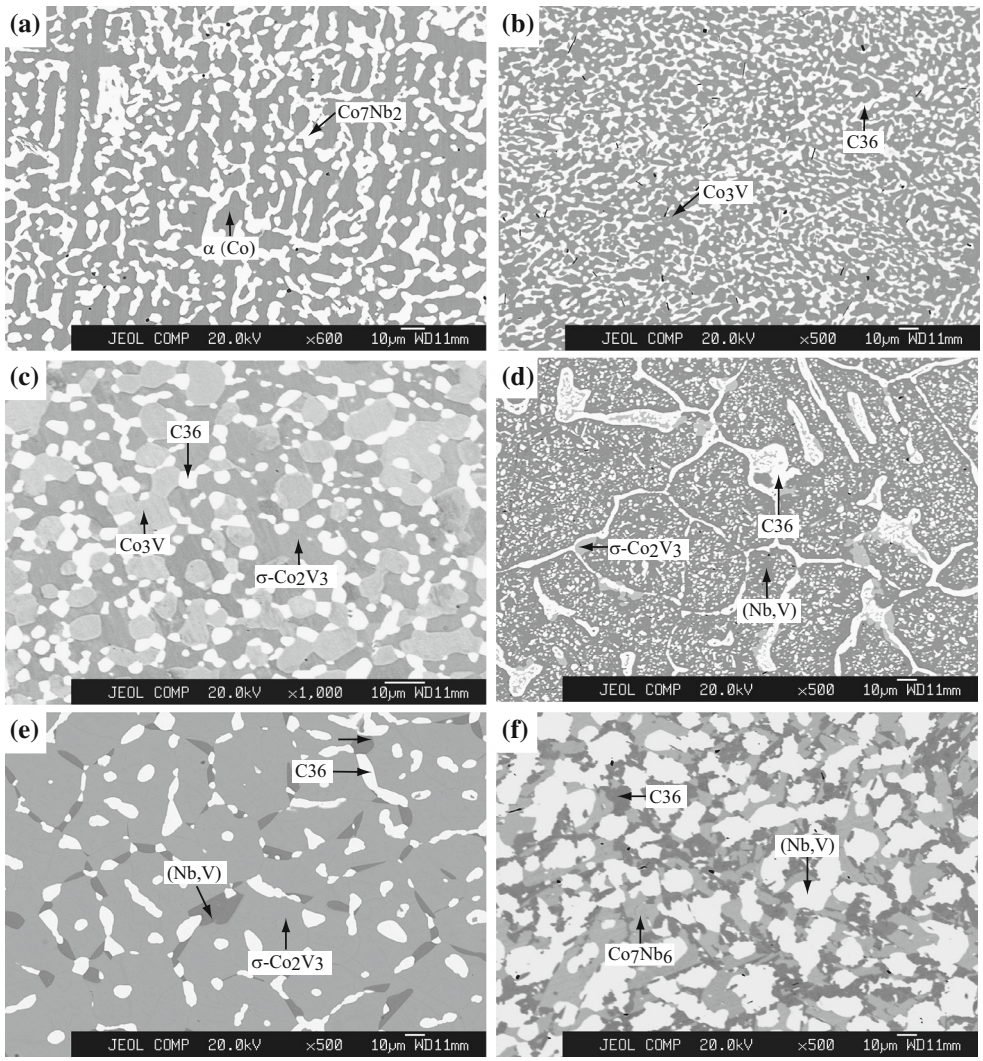

Fig. 2 Typical ternary BSE images obtained from: (a) $Co_{85}Nb_{10}V_5$ (all alloy compositions are giving in at.%) alloy annealed at 1000 °C for 45 days; (b) $Co_{75}Nb_{10}V_{15}$ alloy annealed at 1000 °C for 45 days; (c) $Co_{60}Nb_{10}V_{30}$ alloy annealed at 1000 °C for 45 days; (d) $Co_{20}Nb_{10}V_{70}$ alloy annealed at 1000 °C for 45 days; (e) $Co_{20}Nb_{10}V_{70}$ alloy annealed at 1200 °C for 25 days; (f) $Co_{20}Nb_{30}V_{50}$ alloy annealed at 1200 °C for 25 days

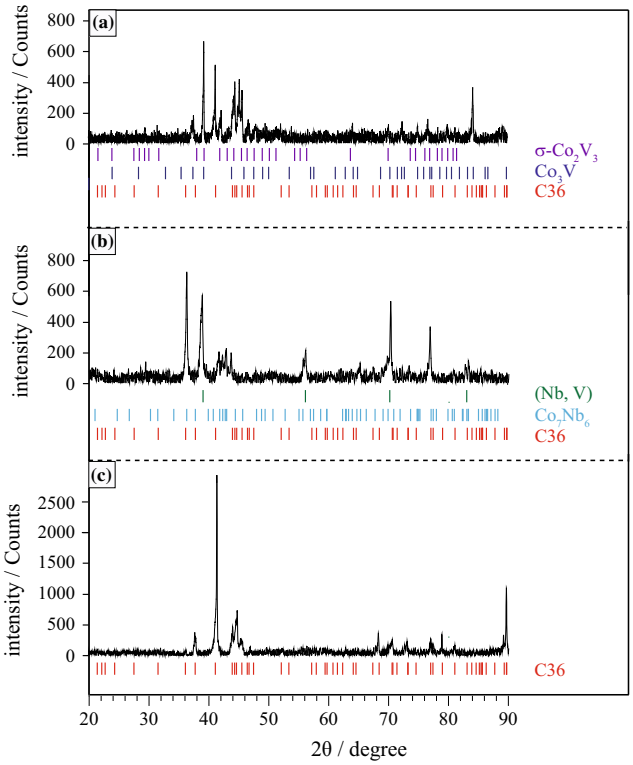

Fig. 3 X-ray diffraction patterns obtained from: (a) $Co_{60}Nb_{10}V_{30}$ alloy annealed at 1000 °C for 45 days; (b) $Co_{25}Nb_{50}V_{25}$ alloy annealed at 1200 °C for 25 days; (c) $Co_{65}Nb_{25}V_{10}$ alloy annealed at 1000 °C for 50 days

$Co_{60}Nb_{10}V_{30}$ alloy by annealing at 1000 °C for 45 days, the three-phase equilibrium (C36 (white) + Co_3V (light gray) + σ-Co_2V_3 (black)) was determined in Fig. 2(c). The structures of three phases were identified by the XRD in Fig. 3(a). It can be seen that the characteristic peaks of the Co_3V phase, σ-Co_2V_3 phase and the C36 Laves phase are well distinguished by different symbols. The three-phase equilibrium (C36 (white) + σ-Co_2V_3 (light gray) + (Nb, V) (black)) was identified in the $Co_{20}Nb_{10}V_{70}$ alloy annealed at 1000 °C for 45 days in Fig. 2(d). The three-phase equilibrium C36 + σ-Co_2V_3 + (Nb, V) was identified in the $Co_{20}Nb_{10}V_{70}$ alloy annealed at 1200 °C for 25 days, as indicated in Fig. 2(e), where σ-Co_2V_3 phase is light gray, the (Nb, V) phase is black and the C36 phase is white. The three-phase equilibrium (Nb, V) (white) + Co_7Nb_6 + (gray) + C36 (black) was observed in the $Co_{25}Nb_{50}V_{25}$ alloy annealed at 1200 °C for 25 days, as illustrated in Fig. 2(f). These three phases were also confirmed by the XRD, as shown in Fig. 3(b).

3.2 Isothermal Sections

The equilibrium compositions of the Co-Nb-V ternary alloys in the present study at 1000 and 1200 °C determined by EPMA are summarized in Tables 2 and 3. Based on the experimental data mentioned above, the isothermal sections at 1000 and 1200 °C were constructed in Fig. 4(a) and (b), respectively. Undetermined three-phase regions have dashed outlines.

In the isothermal section at 1000 °C, as shown in Fig. 4(a), three three-phase regions were experimentally

Table 2 Equilibrium compositions of the Co-Nb-V ternary alloys at 1000 °C determined in the present work

			Equilibria	Composition, at.%					
				Phase 1		Phase 2		Phase 3	
T, °C	Alloys, at.%	Annealed time, days	Phase 1/Phase 2/Phase 3	Nb	V	Nb	V	Nb	V
1000	$Co_{20}Nb_{10}V_{70}$	45	σ-Co_2V_3/C36	4.8	66.0	22.5	44.5	.....	.....
	$Co_{30}Nb_{10}V_{60}$	45	σ-Co_2V_3/C36	2.4	50.8	19.1	31.6	.....	.....
	$Co_{40}Nb_{10}V_{50}$	45	σ-Co_2V_3/C36	1.9	46.3	19.6	26.4	.....	.....
	$Co_{85}Nb_{10}V_5$	45	α-Co/Co_7Nb_2	2.8	7.2	21.2	1.3	.....	.....
	$Co_{75}Nb_{10}V_{15}$	45	α-Co/Co_7Nb_2	7.8	16.8	22.4	5.1	.....	.....
	$Co_{70}Nb_{10}V_{20}$	45	Co_3V/C36	3.2	23.9	21.5	13.8	.....	.....
	$Co_{60}Nb_{10}V_{30}$	45	Co_3V/C36/σ-Co_2V_3	2.1	26.9	19.9	19.4	2.1	37.0
	$Co_{20}Nb_{10}V_{70}$	45	C36/σ-Co_2V_3/(Nb, V)	24.8	46.3	4.6	69.4	2.9	84.4
	$Co_{20}Nb_{30}V_{50}$	45	C36/(Nb, V)	27.7	47.4	12.0	84.4	.....	.....
	$Co_{30}Nb_{65}V_5$	45	Co_7Nb_6/(Nb, V)	51.1	6.0	88.8	3.9	.....	.....
	$Co_{20}Nb_{10}V_{70}$	45	C36/(Nb, V)	31.6	39.6	77.3	19.5	.....	.....
	$Co_{60}Nb_5V_{35}$	50	C36/σ-Co_2V_3	19.9	21.1	1.9	38.9	.....	.....
	$Co_{25}Nb_{50}V_{25}$	50	C36/Co_7Nb_6/(Nb, V)	33.8	34.8	42.5	27.4	78.5	18.0
	$Co_{10}Nb_{50}V_{40}$	50	C36/(Nb, V)	32.1	48.9	66.5	31.9	.....	.....
	$Co_{45}Nb_{40}V_{15}$	50	C36/Co_7Nb_6	31.5	17.8	43.1	13.4	.....	.....
	$Co_{10}Nb_{40}V_{50}$	50	C36/(Nb, V)	31.9	51.5	45.3	53.4	.....	.....
	$Co_{65}Nb_{25}V_{10}$	50	C36	30.4	11.1	.....	.....	.....	.....

Table 3 Equilibrium compositions of the Co-Nb-V ternary alloys at 1200 °C determined in the present work

T, °C	Alloys, at.%	Annealed time, days	Equilibria	Composition, at.%					
				Phase 1		Phase 2		Phase 3	
			Phase 1/Phase 2/Phase 3	Nb	V	Nb	V	Nb	V
1200	$Co_{40}Nb_{10}V_{50}$	25	σ-Co_2V_3/C36	2.7	52.7	18.5	34.1	.....	.....
	$Co_{50}Nb_{10}V_{40}$	25	σ-Co_2V_3/C36	1.6	44.4	16.8	28.8	.....	.....
	$Co_{60}Nb_{10}V_{30}$	25	α (Co)/C36	5.1	31.7	17.7	21.3	.....	.....
	$Co_{75}Nb_{15}V_{10}$	25	α (Co)/C36	2.7	14.9	21.9	4.4	.....	.....
	$Co_{75}Nb_{20}V_5$	25	α (Co)/C36	2.9	12.0	21.7	3.2	.....	.....
	$Co_{85}Nb_{10}V_5$	25	α (Co)/C36	3.6	6.5	22.9	1.4	.....	.....
	$Co_{75}Nb_{10}V_{15}$	25	α (Co)/C36	3.3	18.3	22.3	7.3	.....	.....
	$Co_{70}Nb_{10}V_{20}$	25	α (Co)/C36	2.0	23.4	20.9	12.2	.....	.....
	$Co_{20}Nb_{10}V_{70}$	25	σ-Co_2V_3/C36/(Nb, V)	5.2	65.6	24.2	42.0	5.1	92.5
	$Co_{20}Nb_{30}V_{50}$	25	C36/(Nb, V)	28.9	44.9	21.3	75.7	.....	.....
	$Co_{20}Nb_{50}V_{30}$	25	C36/(Nb, V)	40.0	36.4	76.0	22.1	.....	.....
	$Co_{30}Nb_{50}V_{20}$	25	Co_7Nb_6/(Nb, V)	44.8	21.2	78.6	19.0	.....	.....
	$Co_{30}Nb_{65}V_5$	25	Co_7Nb_6/(Nb, V)	51.3	6.9	94.4	2.7	.....	.....
	$Co_{25}Nb_{50}V_{25}$	25	C36/Co_7Nb_6/(Nb, V)	35.7	30.4	43.2	24.1	78.5	20.4
	$Co_{10}Nb_{50}V_{40}$	25	C36/(Nb, V)	34.5	43.1	60.6	36.9	.....	.....
	$Co_{65}Nb_5V_{30}$	25	α (Co)/C36	3.9	27.2	18.8	20.1	.....	.....
	$Co_{40}Nb_{25}V_{35}$	30	C36	25.8	32.4	.....	.....	.....	.....
	$Co_{65}Nb_{25}V_{10}$	30	C36	29.5	10.4	.....	.....	.....	.....

determined in this work, namely σ-Co_2V_3 + C36 + (Nb, V), σ-Co_2V_3 + Co_3V + C36 and C36 + Co_7Nb_6 + (Nb, V). It should be noted that the non-existent C36 Laves-phase in Co-Nb subsystem appears in the isothermal section of Co-Nb-V ternary system. The C36 phase (Laves-phase) region seen in Fig. 4(a) indicates that the V addition stabilizes this phase at lower temperature. Similarly, the stabilization of the C14 phase (Laves-phase) was also confirmed in Zhao et al.[35] Furthermore, the single phase C36 was substantiated by the XRD, as shown in Fig. 3(c). Figure 4(b) shows the isothermal section at 1200 °C, where two three-phase equilibrium σ-Co_2V_3 + C36 + (Nb, V) and C36 + (Nb, V) + Co_7Nb_6 were experimentally determined in this work.

Comparing these two isothermal sections, we can see that the solubility of Nb in α (Co) and σ-Co_2V_3 phase is limited, the area of α (Co) phase at 1000 °C is smaller than that at 1200 °C. In the isothermal sections at 1000 °C and 1200 °C, the phase of (Nb, V) form the continuous solid solutions, and the solubility of Co is large in the V-rich and Nb-rich side, but small in the middle of (Nb, V) phase. The C36 phase is identified to possess large solubility of V. Considering the position of the C36 phase in the ternary system investigated, it is reasonable to infer that V and Co atoms show the analogous site occupation in that phase. V element does not have the tendency to occupy the position of Co or Nb in the Co_7Nb_6 phase.

4. Conclusions

Two isothermal sections of the Co-Nb-V ternary system at 1000 and 1200 °C were experimentally determined by the means of EPMA and XRD. The obtained experimental results show that (1) the solubility of Nb in α (Co) and σ-Co_2V_3 phases is limited; (2) the phase of (Nb, V) forms the continuous solid solution, and the solubility of Co is large in the V-rich and Nb-rich side; (3) the presence of the single phase C36 at 1000 °C suggests the stabilization at lower temperature and the solubility of V in the phase was identified to be large in this work; (4) V and Co atoms show the analogous site occupation in the phase; (5) V and Co atoms do not show the analogous site occupation in the phase Co_7Nb_6. The newly determined phase equilibria in this system will be very important for the development of the Co-base functional materials and thermodynamic assessment of the Co-Nb-V ternary system.

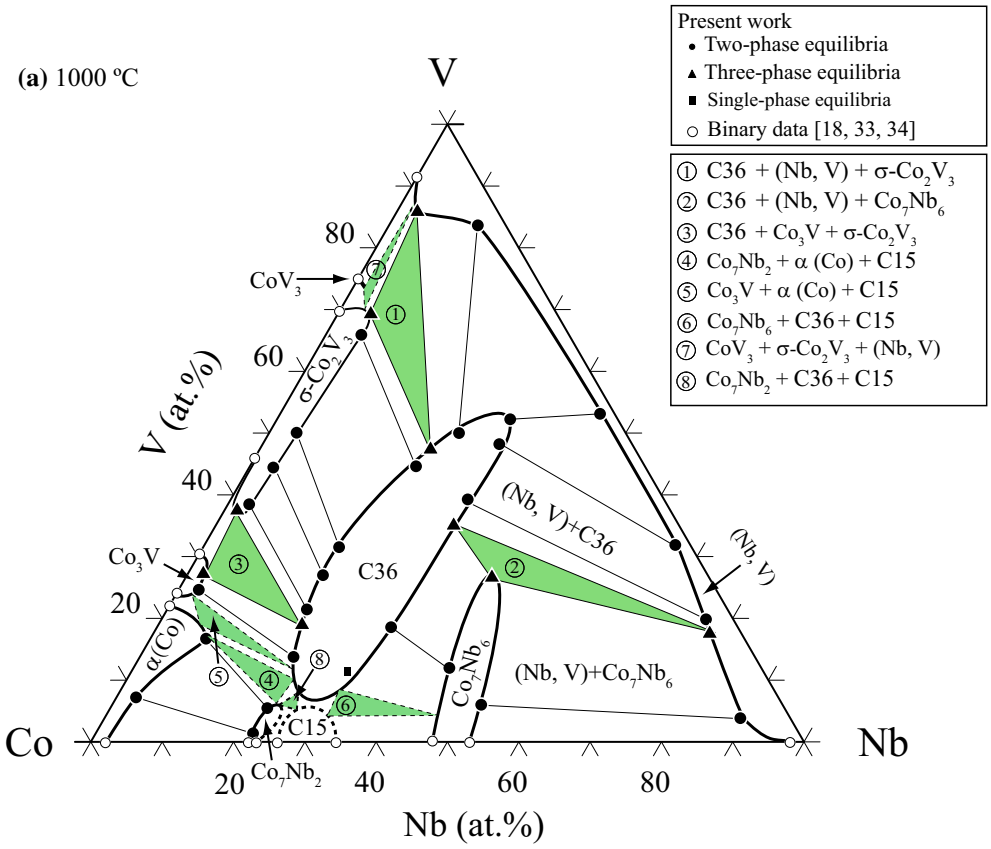

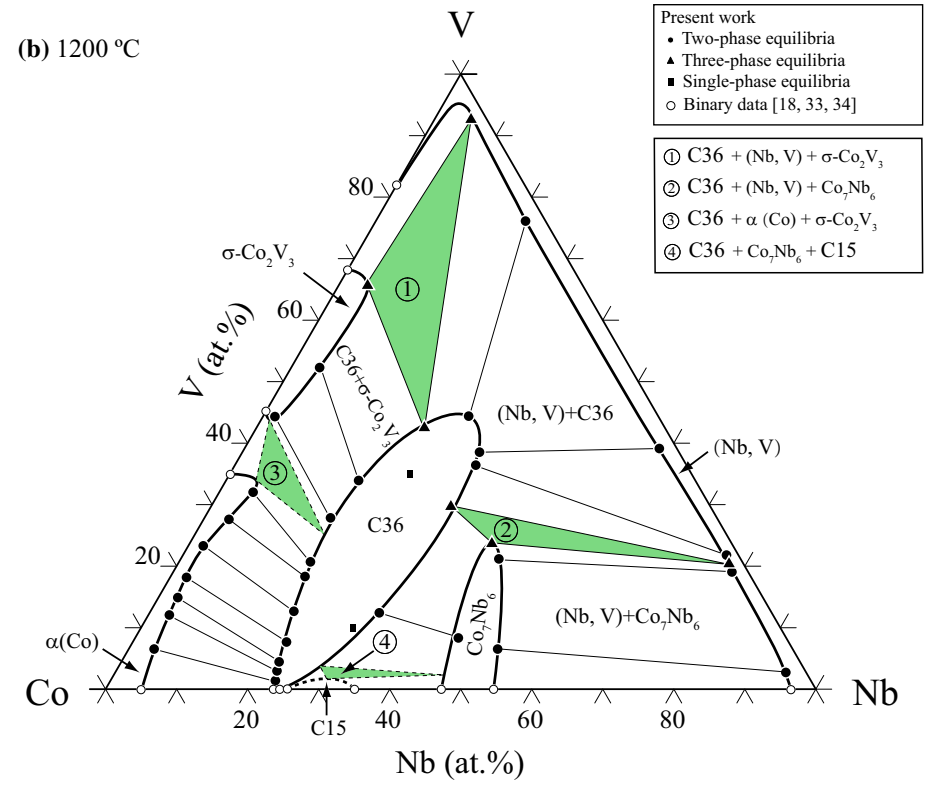

Fig. 4 Experimentally determined isothermal sections of the Co-Nb-V system at: (a) 1000 °C, (b) 1200 °C

Acknowledgments

This work was supported by the National Natural Science Foundation of China (Grant Nos. 51471138 and 51171159) and the Ministry of Education of China (Grant No. 20120121130004). The support from the Ministry of Science and Technology of China (Grant Nos. 2012CB825700 and 2014DFA53040), the Science and Technology Bureau of Xiamen City (Grant No. 3502Z20131153) are also acknowledged.

References

1. C.T. Sims and W.C. Hagel, *The Superalloys-Vital High Temperature Gas Turbine Materials for Aerospace and Industrial Power*, Wiley, New York, 1972, p 145-185
2. H. Chinen, Doctoral Thesis, Tohoku University, 2010
3. K. Shinagawa, T. Omori, K. Oikawa, R. Kainuma, and K. Ishida, Ductility Enhancement by Boron Addition in Co–Al–W High-Temperature Alloys, *Scr. Mater.*, 2009, **61**(6), p 612-615
4. A. Bauer, S. Neumeier, F. Pyczak, and M. Göken, Microstructure and Creep Strength of Different γ/γ′-Strengthened Co-Base Superalloy Variants, *Scr. Mater.*, 2010, **63**(12), p 1197-1200
5. T. Yokokawa, M. Osawa, K. Nishida, T. Kobayashi, Y. Koizumi, and H. Harada, Partitioning Behavior of Platinum Group Metals on the γ and γ′ Phases of Ni-Base Superalloys at High Temperatures, *Scr. Mater.*, 2003, **49**(10), p 1041-1046
6. G.W. Qin, K. Oikawa, M. Sato et al., Co-Mo and Co-Mo-Cr Alloy Thin Films Promising for Magnetic Recording, *IEEE Trans. Magn.*, 2005, **41**(2), p 918-920
7. V. Loo, J. Vrolijk, and G.F. Bastin, Phase Relations and Diffusion Paths in the Ti-Ni-Fe System at 900 C, *J. Less Common Metals*, 1981, **77**(1), p 121-130
8. Z. Wu, Z. Liu, H. Yang et al., Effect of Co Addition on Martensitic Phase Transformation and Magnetic Properties of $Mn_{50}Ni_{40-x}In_{10}Co_x$ Polycrystalline Alloys, *Intermetallics*, 2011, **19**(12), p 1839-1848
9. A. Kostov and D. Živković, Thermodynamic Analysis of Alloys Ti–Al, Ti–V, Al–V and Ti–Al–V, *J. Alloy. Compd.*, 2008, **460**(1), p 164-171
10. J. Sha, H. Hirai, H. Ueno et al., Mechanical Properties of As-cast and Directionally Solidified Nb-Mo-W-Ti-Si In Situ Composites at High Temperatures, *Metall. Mater. Trans.*, 2003, **34**(1), p 85-94
11. W. Köster and E. Wagner, Effect of the Elements Al, Ti, V, Cu, Zn, Sn and Sb on the Polymorphic Transition of the Cobalt, *Z. Metallkd*, 1937, **29**, p 230-232
12. W. Rostoker and A. Yamamoto, A Survey of Vanadium Binary Systems, *Trans. Am. Soc. Metals*, 1954, **46**, p 1136-1167
13. P. Pietrokowsky and P. Duwez, Crystallography of the Sigma-Phase, *Trans. Am. Inst. Min. Metall. Eng.*, 1950, **188**(10), p 1283-1284
14. W.B. Pearson, J.W. Christian, and W. Hume-Rothery, New Sigma-Phases in Binary Alloys of the Transition Elements of the First Long Period, *Nature*, 1951, **167**, p 110
15. A.H. Sully, The Sigma Phase in Binary Alloys of the Transition Elements, *J. Inst. Metals.*, 1951, **80**, p 9
16. W.B. Pearson and J.W. Christian, The Structure of the σ Phase in Vanadium–Nickel Alloys, *Acta Crystallogr. A*, 1952, **5**(2), p 157-162
17. P. Greenfield and P.A. Beck, The Sigma Phase in Binary Alloys, *Trans. AIME*, 1954, **200**, p 253
18. J. Bratberg and B. Sundman, A Thermodynamic Assessment of the Co-V System, *J Phase Equilib.*, 2003, **24**(6), p 495-503
19. W. Köster and W. Mulfinger, The Binary Systems of Co with B, As, Zr, Nb, and Ta, *Z. Metallkd*, 1938, **30**, p 348-350
20. H.J. Wallbaum, The Systems of the Iron Metals with Titanium, Zirconium, Columbium and Tantalum, *Archiv fur das Eisenhiittenwesen*, 1941, **14**, p 521-526
21. H.J. Wallbaum, X-Ray Structure of AB_2 Alloys of Iron with Titanium, Zirconium, Niobium, and Tantalum, *Z. Krist.*, 1941, **103**, p 391-402
22. S. Saito and P.A. Beck, Co-rich Intermediate Phases in the Cb-Co System, *Trans. Met. Soc. AIME*, 1960, **218**, p 670
23. A.K. Shurin and G.P. Dmitrieva, Phase Diagram of the System Chromium-Ruthenium, *Sb. Nauchn. Rab. Inst. Metallofiz. Akad. Nauk Ukr. SSR*, 1964, **18**, p 170-174
24. Y.B. Kuz'ma, A.K. Shurin, G.P. Dmitrieva, and E.I. Gladyshevskii, Crystal Structure of β Phase of the System Co-Nb and Solubility of Silicon in It, *Dopov. Akad. Nauk Ukr. RSR*, 1964, **5**, p 600-603
25. A. Raman, X-Ray Investigation in the Niobium (Columbium)-Cobalt System, *Trans. Metall. Soc. AIME*, 1966, **236**, p 561-565
26. J.K. Pargeter and W. Hume-Rothery, The Constitution of Niobium-Cobalt Alloys, *J. Less Common Metals*, 1967, **12**(5), p 366-374
27. S.K. Bataleva, V.V. Kuprina, V.Y. Markiv et al., Cobalt-Niobium Phase Diagram, *Mosc. Univ. Chem. Bull.*, 1970, **25**(4), p 37-40
28. S.K. Bataleva, V.V. Kuprina, and V.Y. Markiv, Phase Diagrams of the Co-Zr and Co-Nb Systems, *Sbornik Trudov. Moskov. Vech. Met. Inst.*, 1972, **12**, p 467-469
29. L. Kaufman and H. Nesor, Calculation of Superalloy Phase Diagrams: Part III, *Metall. Trans. A*, 1975, **6**(11), p 2115-2122
30. L. Kaufman and H. Nesor, Coupled Phase Diagrams and Thermochemical Data for Transition Metal Binary Systems—II, *CALPHAD*, 1978, **2**(1), p 81-108
31. N.F. Shen, I.P. Jones, and J.N. Pratt, Electron Microscopy of Annealed Rapidly-Cooled Co-Nb Alloys, *Mater. Chem. Phys.*, 1986, **15**(1), p 15-25
32. W. Sprengel, M. Denkinger, and H. Mehrer, Multiphase Diffusion in the Co-Nb and Ni-Nb Systems: Part I, Solid-Solid Phase Equilibria and Growth of Intermetallic Phases, *Intermetallics*, 1994, **2**(2), p 127-135
33. F. Stein, D. Jiang, M. Palm, G. Sauthoff, D. Grüner, and G. Kreiner, Experimental Reinvestigation of the Co–Nb Phase Diagram, *Intermetallics*, 2008, **16**(6), p 785-792
34. K.C.H. Kumar, P. Wollants, and L. Delaey, Thermodynamic Calculation of Nb-Ti-V Phase Diagram, *CALPHAD*, 1994, **18**(1), p 71-79
35. C.C. Zhao, S.Y. Yang, X.J. Liu, and C.P. Wang, Experimental Determination of the Phase Equilibria in the Co-Cr-Ta Ternary System, *J. Alloy. Compd.*, 2014, **608**, p 118-125